

## Qualitative and Quantitative Contrast-Enhanced Ultrasonographic Assessment of Cerulein-Induced Acute Pancreatitis in Dogs

S.Y. Lim, K. Nakamura, K. Morishita, N. Sasaki, M. Murakami, T. Osuga, H. Ohta, M. Yamasaki, and M. Takiguchi

**Background:** Acute pancreatitis (AP) is the most common disease of the canine exocrine pancreas, and accurate noninvasive diagnosis is challenging.

**Hypothesis/Objectives:** To determine the feasibility of using quantitative contrast-enhanced ultrasonography (CEUS) to detect pancreatic perfusional changes in cerulein-induced AP in dogs.

**Animals:** Six adult female Beagles.

**Methods:** Each dog received 2 hours of IV infusion with 7.5 µg/kg/h of cerulein diluted in saline. As control, all dogs received 2 hours of IV infusion of saline 2 weeks before cerulein infusion. CEUS of the pancreas and duodenum were performed before (0 hour), and at 2, 4, 6, and 12 hours after saline and cerulein infusion. Time-intensity curves were created from regions of interest in the pancreas and duodenum. Five perfusional parameters were measured for statistical analysis: time to initial up-slope, peak time, time to wash-out, peak intensity (PI), and area under the curve (AUC).

**Results:** In cerulein-induced AP, pancreatic PI increased at 2 and 4 hours when compared to 0 hour, and at 2, 4, and 6 hours when compared to control. AUC increased at 4 hours when compared to 0 hour, and at 2 and 4 hours when compared to control. Time to wash-out was prolonged at 4 hours when compared to control. For saline control, peak time was faster at 2 hours when compared to 0 hour.

**Conclusions and Clinical Importance:** CEUS parameters PI and AUC can provide useful information in differentiating acute pancreatitis from normal pancreas. Cerulein-induced AP was characterized by prolonged hyperechoic enhancement on CEUS.

**Key words:** Contrast-ultrasound; Inflammation; Pancreas; Perfusion.

Pancreatitis is the most common disease of the canine exocrine pancreas. Although a common consensus has not been reached for its classification, it can generally be divided into acute and chronic presentations.<sup>1,2</sup>

Currently, there is no gold standard in the antemortem diagnosis of pancreatitis in dogs. One should take into account the complete history, physical examination findings, clinicopathologic results, measurement of pancreatic lipase immunoreactivity, radiography, and ultrasound (US) examination of the pancreas for an accurate noninvasive diagnosis of pancreatitis.<sup>3</sup>

US findings in pancreatitis include an enlarged, irregular, or mass-like pancreas with areas of patchy hypoechoic to mixed patterns of echogenicity. The surrounding mesentery may appear hyperechoic with the possible presence of focal abdominal fluid, corrugation of the neighboring duodenum, and ultrasonographic signs of extrahepatic bile duct obstruction.<sup>4,5</sup> US is useful in the diagnosis of acute pancreatitis (AP), but

### Abbreviations:

AP	acute pancreatitis
AUC	area under the curve
CEUS	contrast-enhanced ultrasound
MB	microbubble
MPV	mean pixel value
PI	peak intensity
ROI	region of interest
TIC	time-intensity curve
Tp	peak time
TTU	time to initial up-slope
TTW	time to wash-out
US	ultrasound

has a reported sensitivity of only 68%.<sup>5</sup> An unremarkable US examination does not rule out pancreatitis.<sup>4</sup>

Recently, US contrast agents have been found to provide information on the macro- and microvascularization of abdominal organs such as the liver, spleen, pancreas, and kidney in both human and veterinary patients.<sup>6–13</sup> Sonazoid, a second-generation contrast agent, contains perfluorobutane gas of low solubility encapsulated by a lipid shell, and is highly stable in vivo.<sup>14</sup> When exposed to intermediate acoustic power ( $0.1 < \text{mechanical index} < 0.5$ ),<sup>15</sup> it develops nonlinear resonance, resulting in harmonic signals with minimal destruction, thus providing continuous real-time contrast imaging of longer duration.<sup>15</sup> Subtraction techniques such as pulse inversion imaging, used in contrast-specific imaging modalities, enhance detection of nonlinear resonance from microbubbles (MB) with high sensitivity while suppressing echoes from tissues.<sup>15</sup>

*From the Laboratory of Veterinary Internal Medicine, Graduate School of Veterinary Medicine, Hokkaido University, Hokkaido, Japan (Lim, Sasaki, Murakami, Osuga, Ohta, Yamasaki, Takiguchi); and the Hokkaido University Veterinary Teaching Hospital (Nakamura, Morishita), Graduate School of Veterinary Medicine, Hokkaido University, Hokkaido, Japan.*

*Corresponding author: M. Takiguchi, Laboratory of Veterinary Internal Medicine, Graduate School of Veterinary Medicine, Hokkaido University, Hokkaido 060-0818, Japan; e-mail: mtaki@vetmed.hokudai.ac.jp.*

*Submitted October 21, 2013; Revised December 11, 2013; Accepted January 7, 2014.*

*Copyright © 2014 by the American College of Veterinary Internal Medicine*

*DOI: 10.1111/jvim.12319*

In contrast-enhanced ultrasound (CEUS) studies in people, enhancement of the pancreas is well-correlated with its perfusion, and can differentiate areas of inflammation (hyperechoic enhancement) and necrosis (nonenhancement).<sup>11,12,16,17</sup> The main indications of CEUS in pancreatic diseases in people are AP, neoplasia, and pseudotumors.<sup>11</sup> CEUS has been reported to be comparable to computed tomography for assessment of AP in people.<sup>18,19</sup> These studies have showed the usefulness of CEUS in detection, staging severity, and predicting clinical outcomes of AP. However, studies in dogs with pancreatitis are few. To our knowledge, only 1 report and abstract exist for CEUS study of pancreatitis in dogs.<sup>20,a</sup>

Cerulein, a cholecystokinin analog, when administered at supraphysiologic doses, leads to excessive digestive enzyme secretion resulting in acute edematous pancreatitis.<sup>21–23</sup> Cerulein-induced AP has been studied extensively in animal models because of its rapid induction, lack of invasiveness, high repeatability, high applicability, and AP-like histologic changes.<sup>21–25</sup> This model also allows the investigation of healing and regeneration of damaged tissues after insult termination.<sup>26</sup> US and endoscopic US findings in experimentally induced pancreatitis in dogs have been described.<sup>22,23</sup>

The purpose of this study was to (1) determine the feasibility of using quantitative CEUS to detect pancreatic perfusional changes, with the duodenum as an internal control, in cerulein-induced AP in dogs and (2) describe the patterns of change over time. Pancreatic perfusion after induction of AP was compared to saline controls (before and after saline infusion) as well as before cerulein infusion. It was hypothesized that quantitative CEUS could detect changes in pancreatic perfusion after induction of AP and, if this hypothesis were to be true, quantitative CEUS would have the potential to be an additional tool in diagnosing and monitoring disease progression in canine AP.

## Materials and Methods

Six adult female Beagles, 1–2 years old, and weighing 9.5–11.3 kg were used in this study. The dogs were healthy based on physical examination findings and normal CBC and serum biochemistry (including amylase, lipase, and C-reactive protein). B-mode US identified no evidence of focal or diffuse abnormalities of the pancreas and duodenum in the dogs. All procedures were approved by the Hokkaido University Animal Care and Use Committee.

AP was induced with continuous IV infusion of 7.5  $\mu\text{g/kg/h}$  of cerulein<sup>b</sup> in saline into the cephalic vein at a rate of 3 mL/kg/h for 2 hours.<sup>21–24</sup> The dogs were observed for the presence of clinical signs associated with AP, such as vomiting and diarrhea. Food was withheld for 24 hours after the start of cerulein infusion and then was slowly reintroduced. As control, all animals received a 2-hour IV infusion of saline at 3 mL/kg/h 2 weeks before cerulein treatment.

US and CEUS examinations were performed before (0 hour) and at 2, 4, 6, and 12 hours after the start of saline and cerulein treatments. Scanning was performed under anesthesia with propofol<sup>c</sup> at an induction dosage of 6 mg/kg and a maintenance rate

of 0.4–0.6 mg/kg/min,<sup>27</sup> administered to effect using a syringe pump.<sup>d</sup>

For US examinations, dogs were positioned in left lateral recumbency, and the right pancreatic lobe and descending duodenum adjacent to the right pancreas were identified using an intercostal approach.

During each CEUS examination, a continuous infusion of MB contrast agent<sup>e</sup> was administered at a dosage of 0.05 mL/kg diluted in 5 mL of saline using a syringe pump.<sup>d,28</sup> The infusion was administered through a 21 G butterfly catheter attached to a 22 G IV catheter placed in a separate cephalic vein from that used for propofol infusion. The timer on the US machine and MB contrast agent infusion were started simultaneously. CEUS was performed using the right intercostal approach to image a transverse view of the right pancreatic lobe and descending duodenum adjacent to the right pancreas. The duodenum was imaged with the pancreas to determine its suitability as an internal control. Scanning was done continuously for 7 min from the start of continuous infusion of MB contrast agent, for generation of a time-intensity curve (TIC).

An US scanner<sup>f</sup> with a 7–14 MHz broadband linear probe<sup>g</sup> was used for B-mode ultrasonography. A 5–11 MHz broadband linear probe<sup>h</sup> suitable for pulse subtracting imaging was used for CEUS. Adjustable parameters were optimized during preliminary studies and maintained throughout the experiments. The mechanical index was set at 0.21 for minimal MB destruction, and focus depth was placed below the pancreas. The B-mode and contrast imaging gain were set at 100 dB and 75 dB, respectively. US imaging was set at 30–31 frames/s, and the images were recorded in 40-second cine-loops to a hard disk for additional off-line analysis.

Quantitative analysis of CEUS images was performed using an image analysis system.<sup>i</sup> This system measures intensity using a gray-scale level ranging from 0 to 255 mean pixel value (MPV). One image per second for the first 120 seconds followed by 1 image at an interval of every 10 seconds until 420 seconds from the start of MB contrast agent infusion was analyzed. Tissue intensity was measured for each region of interest (ROI) containing 300–600 pixels,<sup>9,28</sup> placed in the pancreatic parenchyma and duodenal mucosa (Fig 1A). When respiratory motion was present, the ROI was manually adjusted to maintain the same position within the pancreas and duodenum. TICs (Fig 2), depicting the change in tissue intensity over time in the ROI, were created for each CEUS imaging performed before (0 hour), and 2, 4, 6, and 12 hours after saline or cerulein infusion. From these TICs, blood flow velocity as a function of time parameters and blood volume as a function of intensity parameters were evaluated. Measured time parameters included time to initial up-slope (TTU) and peak time (Tp), reflecting wash-in and time to wash-out (TTW), reflecting wash-out of MBs from the ROI. Peak intensity (PI) and area under the curve (AUC) are intensity parameters, the first quantitatively measuring maximum contrast enhancement within the ROI and the second corresponding to the amount of MB flowing through the tissue over a certain time period within the observed ROI. TTU and TTW were defined as the time when the intensity increased to and decreased to 30% of PI, respectively.<sup>28</sup>

A statistical analysis program<sup>j</sup> was used to develop a linear mixed model, with time (0, 2, 4, 6, and 12 hours), treatment (saline versus cerulein), and their interaction as categorical fixed effects, and dog identity as random effect. The *F* test was performed to assess the effect of time and treatment on the values of the measured parameters. Pairwise comparisons between times and between treatments were performed by obtaining least squares means and using Bonferroni correction to account for multiple comparisons. For all analyses, values of *P* < .05 were considered statistically significant.

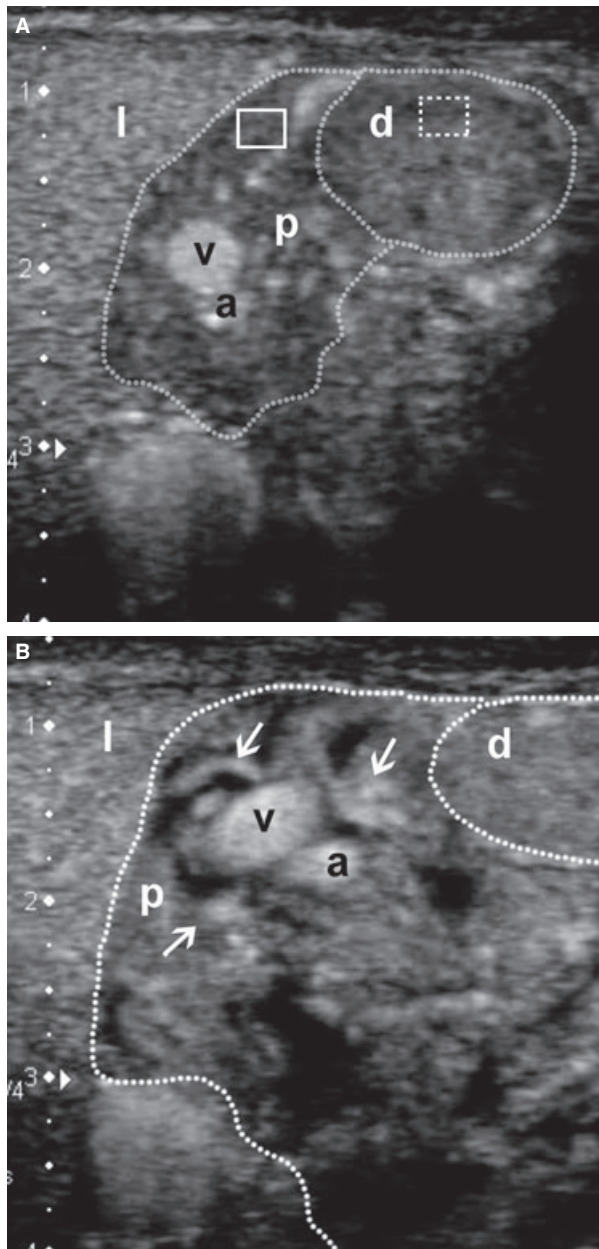


**Fig 1.** CEUS images of the transverse view of the right pancreatic lobe (p), and mucosa of the descending duodenum adjacent to the right pancreas (d) (both outlined by dotted lines) at peak enhancement in a representative dog (dorsal to the left, ventral to the right, medial to the bottom). **(A)** Before cerulein treatment (0 hour). Image acquired 59 seconds after the start of contrast agent infusion showing nonhomogenous enhancement of pancreatic parenchyma and duodenal mucosa. The pancreas is demarcated from the adjacent liver (l). The pancreaticoduodenal artery (a) and vein (v) also are enhanced at this time. ROIs are placed manually in the pancreatic parenchyma (solid box) and duodenal mucosa (dashed box) to measure tissue intensity. **(B)** Two hours after the start of cerulein treatment. Image acquired 58 seconds after contrast agent infusion. The pancreatic parenchyma is more intensely enhanced when compared to 0 hour. The cranial pancreaticoduodenal artery and vein are more prominently enhanced and fine capillaries (arrows) are visible. The swollen pancreatic parenchyma is separated by interlobular fissures and subcapsular edema that were unenhanced.

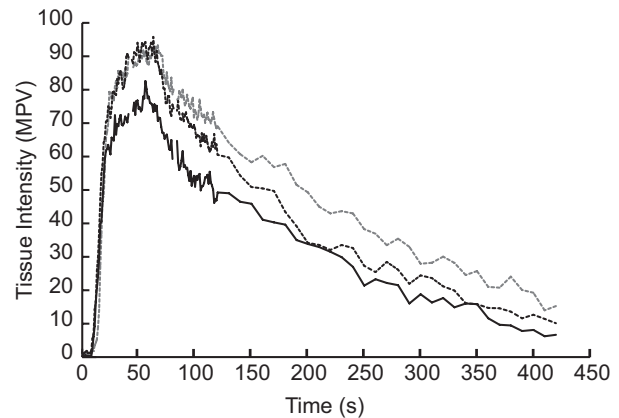


**Fig 2.** TICs showing the mean pixel intensity of the pancreatic parenchyma before (0 hour, solid black line), 2 (dashed black line), and 4 hours (dashed gray line) after cerulein infusion (n = 6). The curves are of the similar shape, but are higher at 2 and 4 hours when compared to 0 hour. The wash-out at 4 hours is more gradual when compared to 0 and 2 hours. MPV, Mean pixel value.

## Results

### Cerulein-Induced AP

AP was induced in all 6 dogs, as shown by presence of clinical signs and increased serum lipase activity after cerulein infusion (data not shown). Within 20 minutes of beginning cerulein infusion, all dogs exhibited clinical signs associated with AP, such as vomiting (6/6), abdominal discomfort (4/6), and diarrhea (2/6). These clinical signs were mostly observed during the 2 hours of cerulein infusion. Vomiting ceased after the end of cerulein infusion. All dogs recovered from AP without complications within 1–2 days, as shown by complete resolution of clinical signs.

### US Findings

In all dogs, pancreatic lesions were most apparent 2–4 hours after the start of cerulein infusion, and included glandular swelling, well-defined interlobular anechoic fissures, and subcapsular anechoic spaces. All dogs showed severe swelling at 2 hours, whereas 3/6 showed severe and 3/6 showed moderate swelling at 4 hours. In all but 1 dog, mild corrugation of the duodenum was seen at different time points after the start of cerulein infusion. With time, the lesions became less severe, and by 12 hours the pancreatic lesions described above were no longer apparent aside from some swelling (2/6 mild, 1/6 moderate). Hyperechoic mesentery was observed in 3/6 dogs at 2 hours and in all dogs at 4 hours. No peripancreatic fluid accumulation was observed at any time point. There were no observable changes in the pancreas or duodenum in saline controls.

### CEUS Findings

At 0 hour (before saline or cerulein infusion), the cranial pancreaticoduodenal artery was enhanced



earliest, followed by the pancreatic parenchyma, and then duodenal mucosa. The increase in tissue enhancement was gradual until it reached PI (Fig 1A), followed by a plateau. Thereafter, there was progressive wash-out of the contrast agent with gradual loss of tissue enhancement. Subjectively, the parenchyma of the pancreas and duodenum could not be seen clearly when the intensity decrease to approximately 30 MPV.

In cerulein treatment, CEUS changes in the pancreas were most apparent 2–4 hours after infusion and became less severe with time. Subjectively, the pancreatic parenchyma showed similar gradual increase in echogenicity, but was more intensely enhanced at PI when compared to 0 hour (before cerulein infusion, Fig 1B). The cranial pancreaticoduodenal artery and vein were more prominent, and fine pancreatic capillaries were visible. The swollen pancreatic parenchyma was separated by anechoic interlobular fissures that were unenhanced. Similarly, subcapsular edema also was unenhanced. The pancreatic parenchyma was hyperechoic for a longer duration with delayed wash-out when compared to 0 hour (before cerulein infusion). There were no observable changes in the wash-in speed or Tp. The order of tissue enhancement remained unchanged from 0 hour (before saline or cerulein infusion) with the pancreas enhancing before the duodenum in all dogs. With saline treatment, Tp was slightly faster 2 hours after the start of saline infusion. There were no other observable changes in pancreatic enhancement. Changes to the intensity or time parameters of the duodenal mucosa after saline or cerulein treatments were not observed.

### Statistical Analysis

Descriptive statistics for the measured parameters, reflecting pancreatic and duodenal perfusion, are summarized in Table 1. For the pancreas, significant interaction between treatment and time was found for PI ( $P = .033$ ). Dogs subjected to cerulein treatment had significantly higher PI at 2 (least squares [LS] means, 101 MPV; 95% confidence interval [CI], 89–113 MPV;  $P = .0026$ ) and 4 hours (LS means, 99 MPV; 95% CI, 88–111 MPV;  $P = .0091$ ) compared to baseline PI at 0 hour (LS means, 83 MPV; 95% CI, 71–94 MPV). Pairwise comparisons of specific treatment-time combinations identified a significant treatment effect at 2 (saline treatment LS means, 78 MPV; 95% CI, 67–90 MPV;  $P < .001$ ), 4 (saline treatment LS means, 79 MPV; 95% CI, 67–90 MPV;  $P < .001$ ), and 6 hours (cerulein treatment LS means, 92 MPV; 95% CI, 80–104 MPV versus saline treatment LS means, 77 MPV; 95% CI, 66–89 MPV;  $P = .033$ ).

Area under the curve for cerulein treatment followed a time course similar to PI. Significant interaction between treatment and time was detected for AUC ( $P = .028$ ). A significant time effect relative to 0 hour was identified at 4 hours (LS means, 19,700 MPV\*s; 95% CI, 16,200–23,100 MPV\*s;  $P = .0013$ ) for cerulein treatment. Pairwise comparisons of specific treatment-time combinations identified a significant

treatment effect at 4 (saline treatment LS means, 12,000 MPV\*s; 95% CI, 8,600–15,500 MPV\*s;  $P < .001$ ) and 6 hours (cerulein treatment LS means, 18,000 MPV\*s; 95% CI, 14,600–21,500 MPV\*s versus saline treatment LS means, 12,600 MPV\*s; 95% CI, 9,100–16,000 MPV\*s;  $P = .0026$ ).

TTW showed significant treatment and time interaction ( $P = .034$ ). A significant difference between the cerulein (LS means, 295 s; 95% CI, 257–333 s;  $P = .034$ ) and saline treatment (LS means, 210 s; 95% CI, 172–248 s) at 4 hours was observed. For saline treatment, significant time effect was found for Tp at 2 hours (LS means, 48 s; 95% CI, 42–54 s;  $P = .026$ ) when compared to 0 hour (LS means, 61 s; 95% CI, 55–66 s). No significant differences were observed for TTU. Measured parameters for the duodenum did not exhibit any significant differences for both saline and cerulein treatments.

### Discussion

AP was successfully induced in this study. Quantitative CEUS detected perfusion changes in the pancreas of dogs with cerulein-induced AP. Significant changes were observed in the pancreas for the intensity parameters (PI, AUC), reflecting increased blood volume,<sup>10,29</sup> within 2–4 hours postinfusion. As a function of blood flow velocity,<sup>10,29</sup> the time parameter TTW was prolonged at 4 hours postcerulein infusion when compared to saline control at 4 hours, and Tp was faster after 2 hours of saline infusion when compared to baseline values (presaline treatment). The intensity parameters of the pancreas normalized to baseline values (precerulein treatment) within 10 hours after termination of cerulein infusion. Although the duodenum showed mild corrugation on B-mode US, no changes in intensity or time parameters were detected on CEUS.

Infusion of supraphysiological doses of cerulein results in the development of acute edematous pancreatitis in many animal models including the dog.<sup>21–25</sup> This noninvasive method produces consistent histologic and B-mode ultrasonographic findings within 2–4 hours of infusion.<sup>22–24</sup> In our study, these B-mode ultrasonographic results were reproducible, and were consistent with previous reports with changes seen most dramatically in the pancreas from 2 to 4 hours after cerulein treatment.

CEUS uses MB, which are blood-pool contrast agents. Although the capillary network is not anatomically visible in CEUS, MB in the microvasculature can be perceived as contrast enhancement with echogenicity dependent on the amount of MB in the ROI.<sup>30</sup> CEUS provides real-time information corresponding with the perfusion dynamics of the pancreas and disease progression in the AP patient.<sup>18</sup> B-mode US provides useful information on the appearance of the pancreas, but it is highly subjective and dependent on the assessment and experience of each ultrasonographer. Quantification of echogenicity on CEUS using TIC provides additional objective assessment of the perfusional changes in the pancreas.

**Table 1.** Least squares means (95% confidence intervals) obtained from the linear mixed model for measured parameters from TICs before (0 hour), 2, 4, 6, and 12 hours after saline and cerulein treatment (n = 6).

Measured Parameters, by Location	Time (hour)											
	Saline Treatment						Cerulein Treatment					
	0	2	4	6	12	0	2	4	6	12		
Pancreas												
PI (MPV)	78 (66–90)	78 (67–90)	79 (67–90)	77 (66–89)	78 (66–90)	83 (71–94)	101 (89–113) <sup>a,c</sup>	99 (88–111) <sup>a,c</sup>	92 (80–104) <sup>b</sup>	86 (74–98)		
AUC	12,200 (8,800–15,700)	13,100 (9,700–16,500)	12,000 (8,600–15,500)	12,600 (9,100–16,000)	12,700 (9,300–16,200)	14,000 (10,600–17,500)	17,000 (13,600–20,500)	19,700 (16,200–23,100) <sup>a,c</sup>	18,000 (14,600–21,500) <sup>a</sup>	15,300 (11,900–18,800)		
MPV*s												
TTU (s)	18 (16–20)	16 (14–18)	18 (16–20)	20 (17–22)	19 (17–21)	15 (13–17)	14 (12–17)	18 (16–20)	17 (14–19)	17 (15–19)		
TP (s)	61 (55–66)	48 (42–54) <sup>d</sup>	64 (58–69)	60 (55–66)	56 (50–62)	58 (52–64)	56 (50–61)	60 (54–65)	60 (55–66)	58 (53–64)		
TTW (s)	232 (192–271)	232 (192–271)	210 (171–249)	238 (199–278)	217 (177–256)	232 (192–271)	230 (191–269)	295 (256–334) <sup>a</sup>	288 (250–326)	243 (204–283)		
Duodenum												
PI (MPV)	70 (55–79)	75 (63–87)	70 (57–82)	71 (59–83)	74 (62–86)	77 (65–89)	81 (69–93)	78 (66–90)	85 (73–97)	75 (63–87)		
AUC	9,000 (6,000–12,000)	9,900 (7,000–12,900)	9,000 (6,000–12,000)	10,100 (7,200–13,100)	10,000 (7,000–12,900)	11,700 (8,700–14,600)	11,000 (8,000–14,000)	12,300 (9,400–15,300)	13,300 (10,300–16,200)	11,500 (8,500–14,400)		
MPV*s												
TTU (s)	21 (17–23)	19 (16–21)	20 (19–23)	23 (20–25)	22 (19–24)	17 (15–20)	18 (15–20)	19 (16–21)	18 (16–21)	21 (19–24)		
TP (s)	63 (58–68)	58 (53–63)	62 (57–66)	65 (60–70)	61 (56–66)	62 (58–67)	51 (47–56)	57 (52–62)	60 (55–65)	59 (54–64)		
TTW (s)	193 (144–241)	197 (149–245)	182 (134–230)	200 (152–248)	218 (170–266)	208 (160–256)	171 (123–219)	218 (170–266)	218 (170–266)	225 (177–273)		

PI, Peak intensity; AUC, Area under the curve; TTU, Time to initial up-slope; TP, Peak time; TTW, Time to wash-out; MPV, Mean pixel value.

<sup>a</sup>Significant ( $P < .01$ ) treatment effect.

<sup>b</sup>Significant ( $P < .05$ ) treatment effect.

<sup>c</sup>Significant ( $P < .01$ ) time effect when compared to 0 hour.

<sup>d</sup>Significant ( $P < .05$ ) time effect when compared to 0 hour.

CEUS can be performed using bolus injection or continuous infusion.<sup>6–10,13,28</sup> Rapid enhancement with fast wash-out of the tissue is seen with bolus injection. In contrast, continuous infusion provides gradual enhancement that may be more useful in detecting tissue perfusional changes.<sup>28</sup>

In this study, the increase in intensity parameters can be attributed to microvascular changes seen in the inflamed pancreas. Previous studies showed that pancreatic microvascular changes in cerulein-induced AP are seen within 2 hours of cerulein infusion, and include gross reduction in the number of capillaries and dilatation of the remaining microvasculature.<sup>24,31</sup> In 1 study using scanning and transmission electron microscopy to demonstrate microvascular derangements, capillaries with obliterated ends and irregular arrangements were observed.<sup>24</sup> Previous CEUS studies in both the human and veterinary medical literature showed increased echogenicity in the inflamed pancreatic parenchyma.<sup>12,a</sup> Increased pancreatic PI in cerulein-induced AP could be because of accumulation of trapped MBs in the obliterated ends of the capillaries in addition to MB flowing into the pancreas. Slower wash-out of these trapped MBs resulted in prolonged TTW and higher AUC values corresponding with visually prolonged hyperechoic enhancement of the inflamed pancreas. In this study, the increase in intensity parameters therefore reflects the increased blood volume in the inflamed pancreas that not only is because of hyperemia,<sup>32</sup> but to some extent to congestion as evidenced by prolonged wash-out of the contrast agent. In contrast, saline infusion did not increase pancreatic blood flow as demonstrated by unchanged values of the intensity parameters, PI and AUC.

In this study, faster Tp at 2 hours postsaline infusion could be because of increased pancreatic circulation from fluid therapy.<sup>33</sup> In the pancreas of cerulein-induced AP, Tp at 2 hours was slower than saline control, but did not differ from 0 hour (precerulein treatment). One would expect Tp to be delayed when compared to 0 hour (precerulein treatment) because of slower velocity of blood flow in dilated and tortuous blood vessels<sup>34</sup> because more time is needed for MB to accumulate to PI. However, these effects could have been countered by the simultaneous infusion of saline with cerulein.

In contrast to a previous report with no secondary duodenal lesions seen on B-mode US,<sup>22</sup> corrugation of the duodenum was seen at different times postcerulein infusion in this study. However, no changes in CEUS were seen in the duodenum for both intensity and time parameters with cerulein or saline treatment although a similar pattern of decreased Tp was seen at 2 hours postsaline infusion. This could be explained by the absence of microcirculatory derangements in the duodenum from the local inflammatory effects of pancreatitis, probably because of the short duration of cerulein infusion in this study. Presence of duodenal corrugation also is a nonspecific US finding that could be present because of various diseases such as

pancreatitis, enteritis, or peritonitis.<sup>35</sup> Furthermore, improvements in ultrasound technology and presence of observer bias because of lack of blinding to treatments (saline or cerulein infusion) may have contributed to detection of duodenal corrugation in this study.

A few limitations were present in this study. Firstly, cerulein-induced AP only results in a mild form of pancreatitis that does not lead to necrosis.<sup>22,25,26</sup> This may explain the difference between CEUS findings in this study and those previously reported in naturally occurring pancreatitis in dogs. This study identified a hyperperfused pancreas, whereas the previous study disclosed hypoperfused or nonenhanced lesions within the pancreas.<sup>20</sup> The ultrasonographic appearance of interlobular edema in this pancreatitis model also is not seen commonly in naturally occurring pancreatitis in dogs.<sup>22</sup> This suggests that this model may not completely reflect the pathogenesis of clinical pancreatitis, or that animals rarely are presented this soon after the onset of inflammation. Additional research in the application of CEUS in detecting naturally occurring pancreatitis and in differentiating focal lesions in pancreatic cancer and mass-forming pancreatitis is warranted. Secondly, because of the short time intervals between subsequent CEUS examinations, pancreatic biopsy could not be performed in this study without causing more inflammation, therefore confounding the effects of cerulein treatment alone.

CEUS applications in abdominal tumors and pancreatic masses evaluate the perfusional differences in the suspicious region from surrounding macroscopically normal regions.<sup>6,7,16,17,29</sup> However, in pancreatitis, a visually normal pancreatic area for internal control is difficult to identify. Thus, in this study, the descending duodenum was imaged with the pancreas to determine its suitability as an internal control. No CEUS changes were observed in the duodenum in this study. As previously reported, PI of the canine pancreas is only slightly higher than that of the duodenum on CEUS with continuous infusion of contrast MB.<sup>28</sup> Thus, real-time visual comparison of the pancreatic parenchyma with the duodenal mucosa for increased hyperechogenicity during the CEUS examination could be done.

In conclusion, CEUS can be used in the dog for detecting microvascular derangements as a possible sign of pancreatic inflammation. Quantifying the intensity parameters, namely PI and AUC, as a function of blood volume can provide valuable information in differentiating acute edematous pancreatitis from normal pancreatic tissue. Cerulein-induced AP was characterized by prolonged hyperechoic enhancement on CEUS.

## Footnotes

<sup>a</sup> Gaschen L, Schur D, Kearney M. Contrast harmonic ultrasound imaging of the normal pancreas and pancreatitis in dogs. Proceedings of ACVR Annual Scientific Meeting 2007 Nov 27–Dec 1; Chicago, IL

- <sup>b</sup> Caerulein; Bachem AG, Bubendorf, Switzerland  
<sup>c</sup> Propofol Mylan; Mylan Inc, Canonsburg, PA  
<sup>d</sup> Top-5300; Top, Tokyo, Japan  
<sup>e</sup> Sonazoid; Daiichi-Sankyo, Tokyo, Japan  
<sup>d</sup> Top-5300; Top  
<sup>f</sup> Aplio XG; Toshiba Medical Systems, Tochigi, Japan  
<sup>g</sup> PLT-1204 AT; Toshiba Medical Systems  
<sup>h</sup> PLT-704 AT; Toshiba Medical Systems  
<sup>i</sup> ImageJ; US National Institutes of Health, Bethesda, MD  
<sup>j</sup> JMP Pro 10; SAS Institute Inc, Cary, NC

## Acknowledgments

This work was performed at Hokkaido University, Hokkaido, Japan and was partially supported by the Grants-in-Aid for Scientific Research (No. 23580436) from the Japan Society for the Promotion of Science (M.T.). Parts of this paper were presented at the 9th Japanese College of Veterinary Internal Medicine Meeting, Yokohama, Japan, 2013 and 2013 American College of Veterinary Internal Medicine Forum, Seattle, WA. The authors thank Dr Yoichi Ito for assistance with the statistical analysis.

**Conflict of Interest Declaration:** The authors disclose no conflict of interest.

## References

- Mansfield C. Acute pancreatitis in dogs: Advances in understanding, diagnostics, and treatment. *Top Companion Anim Med* 2012;27:123–132.
- Watson P. Chronic pancreatitis in dogs. *Top Companion Anim Med* 2012;27:133–139.
- Xenoulis PG, Steiner JM. Canine and feline pancreatic lipase immunoreactivity. *Vet Clin Pathol* 2012;41:312–324.
- Nyland T, Mattoon J, Herrgesell E, et al. Pancreas. In: Nyland T, Mattoon J, eds. *Small Animal Diagnostic Ultrasound*, 2nd ed. Philadelphia, PA: WB Saunders Co; 2002:144–157.
- Hess RS, Saunders HM, Van Winkle TJ, et al. Clinical, clinicopathologic, radiographic, and ultrasonographic abnormalities in dogs with fatal acute pancreatitis: 70 cases (1986–1995). *J Am Vet Med Assoc* 1998;213:665–670.
- Nakamura K, Takagi S, Sasaki N, et al. Contrast-enhanced ultrasonography for characterization of canine focal liver lesions. *Vet Radiol Ultrasound* 2010;51:79–85.
- Nakamura K, Sasaki N, Murakami M, et al. Contrast-enhanced ultrasonography for characterization of focal splenic lesions in dogs. *J Vet Intern Med* 2010;24:1290–1297.
- Johnson-Neitman JL, O'Brien RT, Wallace JD. Quantitative perfusion analysis of the pancreas and duodenum in healthy dogs by use of contrast-enhanced ultrasonography. *Am J Vet Res* 2012;73:385–392.
- Waller KR, O'Brien RT, Zagzebski JA. Quantitative contrast ultrasound analysis of renal perfusion in normal dogs. *Vet Radiol Ultrasound* 2007;48:373–377.
- Haers H, Daminet S, Smets PM, et al. Use of quantitative contrast-enhanced ultrasonography to detect diffuse renal changes in Beagles with iatrogenic hypercortisolism. *Am J Vet Res* 2013;74:70–77.
- D'Onofrio M, Zamboni G, Faccioli N, et al. Ultrasonography of the pancreas. 4. Contrast-enhanced imaging. *Abdom Imaging* 2007;32:171–181.
- Golea A, Badea R, Socaciu M, et al. Quantitative analysis of tissue perfusion using contrast-enhanced transabdominal ultrasound (CEUS) in the evaluation of the severity of acute pancreatitis. *Med Ultrason* 2010;12:198–204.
- Okada M, Hoffmann CW, Wolf KJ, et al. Bolus versus continuous infusion of microbubble contrast agent for liver US: Initial experience. *Radiology* 2005;237:1063–1067.
- Sontum PC. Physicochemical characteristics of Sonazoid, a new contrast agent for ultrasound imaging. *Ultrasound Med Biol* 2008;34:824–833.
- Correas JM, Bridal L, Lesavre A, et al. Ultrasound contrast agents: Properties, principles of action, tolerance, and artifacts. *Eur Radiol* 2001;11:1316–1328.
- D'Onofrio M, Zamboni G, Tognolini A, et al. Mass-forming pancreatitis: Value of contrast-enhanced ultrasonography. *World J Gastroenterol* 2006;12:4181–4184.
- Badea R, Seicean A, Diaconu B, et al. Contrast-enhanced ultrasound of the pancreas—a method beyond its potential or a new diagnostic standard? *J Gastrointest Liver Dis* 2009;18:237–242.
- Ripollés T, Martínez MJ, López E, et al. Contrast-enhanced ultrasound in the staging of acute pancreatitis. *Eur Radiol* 2010;20:2518–2523.
- Rickes S, Uhle C, Kahl S, et al. Echo enhanced ultrasound: A new valid initial imaging approach for severe acute pancreatitis. *Gut* 2006;55:74–78.
- Shanaman MM, Schwarz T, Gal A, et al. Comparison between survey radiography, B-mode ultrasonography, contrast-enhanced ultrasonography and contrast-enhanced multi-detector computed tomography findings in dogs with acute abdominal signs. *Vet Radiol Ultrasound* 2013;54:591–604.
- Renner IG, Wisner JR Jr. Ceruletide-induced acute pancreatitis in the dog and its amelioration by exogenous secretin. *Int J Pancreatol* 1986;1:39–49.
- Lamb CR, Simpson KW. Ultrasonographic findings in cholecystokinin-induced pancreatitis in dogs. *Vet Radiol Ultrasound* 1993;36:139–145.
- Morita Y, Takiguchi M, Yasuda J, et al. Endoscopic and transcutaneous ultrasonographic findings and grey-scale histogram analysis in dogs with caerulein-induced pancreatitis. *Vet Q* 1998;20:89–92.
- McEntee G, Leahy A, Cottell D, et al. Three-dimensional morphological study of the pancreatic microvasculature in caerulein-induced experimental pancreatitis. *Br J Surg* 1989;76:853–855.
- Chan YC, Leung PS. Acute pancreatitis: Animal models and recent advances in basic research. *Pancreas* 2007;34:1–14.
- Su KH, Cuthbertson C, Christophi C. Review of experimental animal models of acute pancreatitis. *HPB (Oxford)* 2006;8:264–286.
- Ilkiw JE. Other potentially useful new injectable anesthetic agents. *Vet Clin North Am Small Anim Pract* 1992;22:281–289.
- Lim SY, Nakamura K, Morishita K, et al. Qualitative and quantitative contrast enhanced ultrasonography of the pancreas using bolus injection and continuous infusion methods in normal dogs. *J Vet Med Sci* 2013;75:1601–1607. doi:10.1292/jvms.13-0199
- Kersting S, Konopke R, Kersting F, et al. Quantitative perfusion analysis of transabdominal contrast-enhanced ultrasonography of pancreatic masses and carcinomas. *Gastroenterology* 2009;137:1903–1911.
- Cosgrove D, Eckersley R. Contrast-enhanced ultrasound: Basic physics and technology overview. In: Lencioni R, ed. *Enhancing the Role of Ultrasound with Contrast Agents*. Milan, Italy: Springer; 2006:3–14.

31. Gress TM, Arnold R, Adler G. Structural alterations of pancreatic microvasculature in cerulein-induced pancreatitis in the rat. *Res Exp Med* 1990;190:401–412.
32. Klar E, Schratt W, Foitzik T, et al. Impact of microcirculatory flow pattern changes on the development of acute edematous and necrotizing pancreatitis in rabbit pancreas. *Dig Dis Sci* 1994;39:2639–2644.
33. Solanki NS, Barreto SG. Fluid therapy in acute pancreatitis. A systematic review of literature. *JOP* 2011;12:205–208.
34. Hall J. Overview of the circulation: Biophysics of pressure, flow, and resistance. In: Hall J, ed. *Guyton and Hall Textbook of Medical Physiology*, 12th ed. Philadelphia, PA: WB Saunders Co; 2011:157–166.
35. Moon ML, Biller DS, Armbrust LJ. Ultrasonographic appearance and etiology of corrugated small intestine. *Vet Radiol Ultrasound* 2003;44:199–203.